

## Design of a Small Controlled Reception Pattern Antenna Array With a Single-Layer Coupled Feed Structure for Enhanced Bore-Sight Gain and a Matching Bandwidth

Jun Hur, Hosung Choo & Gangil Byun

To cite this article: Jun Hur, Hosung Choo & Gangil Byun (2017): Design of a Small Controlled Reception Pattern Antenna Array With a Single-Layer Coupled Feed Structure for Enhanced Bore-Sight Gain and a Matching Bandwidth, Electromagnetics, DOI: [10.1080/02726343.2017.1330589](https://doi.org/10.1080/02726343.2017.1330589)

To link to this article: <http://dx.doi.org/10.1080/02726343.2017.1330589>



Published online: 29 Jun 2017.



Submit your article to this journal [↗](#)



Article views: 9



View related articles [↗](#)



View Crossmark data [↗](#)



# Design of a Small Controlled Reception Pattern Antenna Array With a Single-Layer Coupled Feed Structure for Enhanced Bore-Sight Gain and a Matching Bandwidth

Jun Hur<sup>a</sup>, Hosung Choo<sup>a</sup>, and Gangil Byun<sup>b</sup>

<sup>a</sup>School of Electronic and Electrical Engineering, Hongik University, Seoul, Korea; <sup>b</sup>Research Institute of Science and Technology, Hongik University, Seoul, Korea

## ABSTRACT

This article proposes the design of a controlled reception pattern antenna (CRPA) array with a single-layer coupled feed structure to improve the radiation gain and a matching bandwidth. Each array element consists of a feeding patch and an outer radiating loop printed on a thick ceramic substrate with a high dielectric constant. The loop is capacitively coupled to the patch and the coupling strength is adjusted by varying the gap distance. Antenna characteristics are measured in a full anechoic chamber, and an equivalent circuit is built to verify the operating principle. The results demonstrate that the proposed structure is more suitable to enhance the gain and bandwidth compared to a conventional patch antenna in small CRPA arrays.

## ARTICLE HISTORY



Received 24 November 2016  
Accepted 27 April 2017

## KEYWORDS

Adaptive array; capacitively coupled feed; controlled reception pattern antenna (CRPA) array; GPS array

## 1. Introduction

Controlled reception pattern antenna (CRPA) arrays have been widely used in the global positioning system (GPS) to minimize performance degradation due to intentional jammers and multipath effects in urban environments. These effects can be mitigated by steering pattern nulls toward the directions of unwanted signals, while maintaining higher radiation gain in the direction of satellites (Byun et al., 2015; Zhang & Amin, 2011; Lambert et al., 2009; Ngamjanyaporn et al., 2005). To improve the capability of this null steering operation, high radiation gain without a pattern distortion is required for individual array elements. Thus, a lot of effort has been made to increase the directivity in the upper hemisphere using high-directive antenna structures, such as quadrifilar helix and cavity-backed antennas (Chew & Saunders, 2002; Hebib et al., 2011; Qu et al., 2010; Bayderkhani et al., 2015; Sun & Fay, 2006; Qu et al., 2009); however, their bulky size is not suitable for small CRPA arrays. Although microstrip patch antennas have gained popularity due to low profile characteristics, it is difficult to maintain a high radiation gain in the entire frequency band because of their narrow matching bandwidth. To broaden the matching bandwidth, various approaches are applied to microstrip patch antennas, e.g., an aperture-coupled feed (Ramirez et al., 2011), a proximity-coupled feed (Guo et al., 2009), and an external matching circuit

**CONTACT** Gangil Byun  [kylebyun@gmail.com](mailto:kylebyun@gmail.com)  Research Institute of Science and Technology, Hongik University, 94 Wausan-ro, Mapo-gu, Seoul 04066, Korea.

Color versions of one or more of the figures in the article can be found online at [www.tandfonline.com/uemg](http://www.tandfonline.com/uemg).

(Kaya & Yuksel, 2007). However, these approaches often require an additional layer for the feeding network, which increases the design complexity when applied to small arrays. Therefore, in-depth considerations are desired to broaden matching bandwidths without increasing the design complexity.

In this article, the design of a small CRPA array is proposed to improve the radiation gain and the matching bandwidth using a capacitively coupled feed with a thick high-dielectric ceramic substrate. The proposed array consists of three identical elements, and each element is composed of an inner feeding patch and an outer radiating loop placed in the same layer. The loop is capacitively coupled to the patch, and the coupling strength is adjusted by the gap distance. This single-layer coupled feed structure allows the antenna to maintain better impedance matching and radiation efficiency by confining electromagnetic (EM) fields in proximity to the radiating loop, which also helps to minimize the mutual coupling effect in a small array. A ground slot is then inserted into a ground platform to further reduce the coupling effect, and two corners of the patch and the loop are truncated to achieve circular polarization (CP) properties. To verify the effectiveness of the proposed coupled feed structure in terms of the radiation gain and the bandwidth, its antenna characteristics are compared to a conventional patch antenna with a coaxial feed by varying the substrate thickness. We also observe the near EM fields and build an equivalent circuit model to verify the operating principle of the antenna. The results demonstrate that the proposed coupled feed structure is suitable for small CRPA arrays with the enhanced bore-sight gain and a broader matching bandwidth.

## 2. Proposed antenna design

Figure 1 shows the proposed CRPA array with a radius of  $r_2$ , and the array is arranged on a circular ground platform with a radius of  $r_1$ . The array consists of three identical elements and is printed on a thick ceramic substrate with a high dielectric constant ( $\epsilon_r = 20$ ,  $\tan \delta = 0.004$ ). Each array element is composed of an inner feeding patch and an outer radiating loop placed in the same layer. The radiating loop has a width of  $w_2$ , and its total length is designed to be about one wavelength in the GPS L1 band. The loop is then capacitively coupled to the feeding patch, the edge length of which is determined by the parameter  $w_1$ . To achieve CP properties, two corners of the patch and the loop are truncated by  $t_1$  and  $t_2$ , respectively, and the coupling strength between the patch and the loop is adjusted by varying the gap distance  $g$ . This single-layer coupled feed structure allows the antenna to maintain a higher radiation gain for thicker substrates. In addition, it helps to confine strong EM fields in proximity to the radiating loop, which results in a reduced mutual coupling effect. The mutual coupling strength is further reduced by inserting a ground slot with width  $s_1$  and length  $s_2$  to suppress the surface currents induced on the circular ground platform (Lee et al., 2015).

Detailed design parameters are optimized by a genetic algorithm in conjunction with the FEKO EM simulator (FEKO, 2015), and the optimized values are listed in Table 1. As can be seen, the antenna has a narrow gap  $g$  of 0.5 mm for strong capacitive coupling and a thick substrate with a thickness ( $h$ ) of 8 mm to improve both the radiation gain and the matching bandwidth.

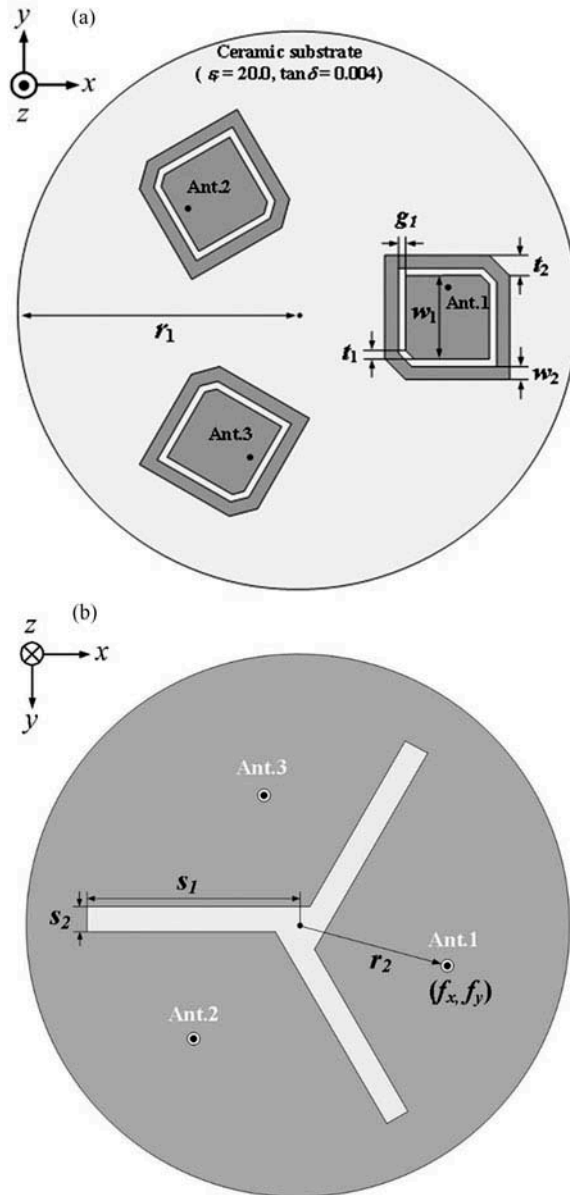


**Figure 1.** Geometry of the proposed CRPA array: (a) Top view, (b) Bottom view.

### 3. Measurement and analysis

Figure 2(a) shows a photograph of the proposed array printed on the ceramic substrate, and Figure 2(b) presents a printed circuit board (PCB) that includes the ground slot and coplanar waveguides with a  $50\text{-}\Omega$  characteristic impedance. The PCB is used as the ground platform by coating its surface with copper ( $\sigma = 5.8 \times 10^7$ ). Then the array is connected to the PCB via feed pins, and antenna characteristics, such as the reflection coefficients, bore-sight gain, axial ratio (AR), and radiation patterns, are

**Table 1.** Optimized values of the proposed array

parameters	Values
$w_1$	13.2 mm
$w_2$	2.5 mm
$g_1$	0.5 mm
$t_1$	1.3 mm
$t_2$	3 mm
$s_1$	9.5 mm
$s_2$	45 mm
$r_1$	60 mm
$r_2$	36 mm
$h$	8 mm
$(f_x, f_y)$	(36, 5.6)

measured in a full anechoic chamber. Figure 3(a) shows simulated reflection coefficients specified by a dash dotted line in comparison with measured results of the three array elements (Ant. 1, Ant. 2, and Ant. 3), which are indicated by solid, dashed, and dotted lines. The three elements have almost identical simulated values of  $-12.8$  dB at 1.5754 GHz because they are arranged symmetrically with respect to the center of the array. The measured reflection coefficients are  $-11.1$ ,  $-11$ , and  $-9.8$  dB at 1.5754 GHz, and the measured 10-dB matching bandwidths are 23, 26, and 23 MHz for Ant. 1, Ant. 2, and Ant. 3, respectively. These results agree well with the simulated bandwidth of 25 MHz, which includes the entire GPS L1 band ( $1,575.4 \text{ MHz} \pm 12 \text{ MHz}$ ). Figure 3(b) presents the mutual coupling between Ant. 1, Ant. 2, and Ant. 3. The array has an inter-element spacing of 63 mm ( $0.3\lambda$ ), and the simulated coupling strength is  $-16.7$  dB at 1.5754 GHz. The measured coupling strengths, denoted as  $|S_{21}|$ ,  $|S_{31}|$ , and  $|S_{32}|$ , are indicated by solid, dashed, and dotted lines, and their values are  $-15.1$ ,  $-14.7$ , and  $-14.7$  dB, respectively.

Figure 4 shows the radiation patterns of the three array elements in the  $zx$ - and  $zy$ -planes at 1.5754 GHz. The simulated patterns have the bore-sight gain of 1.4 dBic, and their average half-power beamwidths (HPBW) are  $69.8^\circ$  ( $zx$ -plane) and  $70.9^\circ$  ( $zy$ -plane). The measured radiation patterns agree well with the simulated data, and Ant. 1, Ant. 2, and Ant. 3 have similar bore-sight gains of 2.1, 2, and 2.4 dBic with average HPBW of  $70.2^\circ$  and  $75.4^\circ$  in the  $zx$ - and  $zy$ -planes, respectively. As can be seen, the antenna does not exhibit any serious pattern distortion in the upper hemisphere with HPBW greater than  $65^\circ$ , which is suitable for use in CRPA applications.

Figure 5 shows the measured bore-sight gain of Ant. 1 in comparison with simulation. The dashed line indicates the simulated results, and the measured data are represented by the solid line and “+” markers. The measured bore-sight gain of the antenna is greater than 0 dBic from 1.49 to 1.62 GHz, and the peak value is 2.37 dBic at 1.5754 GHz, which agrees well with the simulated value of 1.4 dBic. Figure 6 shows the AR of the antenna at  $\theta = 0^\circ$ . The AR is calculated from  $\theta$ - and  $\phi$ -components of the electric fields, denoted as  $E_\theta$  and  $E_\phi$ , in the bore-sight direction, and the measured and simulated AR values are 1.6 and 1.2 dB at 1.5754 GHz. Since the phase difference between  $E_\theta$  and  $E_\phi$  is  $-85.6^\circ$ , the antenna has the right-hand circular polarization with the 3-dB AR bandwidths of 6 and 7 MHz for the measurement and simulation, respectively.

To verify the advantage of the proposed coupled feed structure, we observe variations of the 10-dB matching bandwidth and the bore-sight gain according to the substrate thickness ( $h$ ). The thickness is varied from 3 to 12 mm at an interval of 1 mm, and the

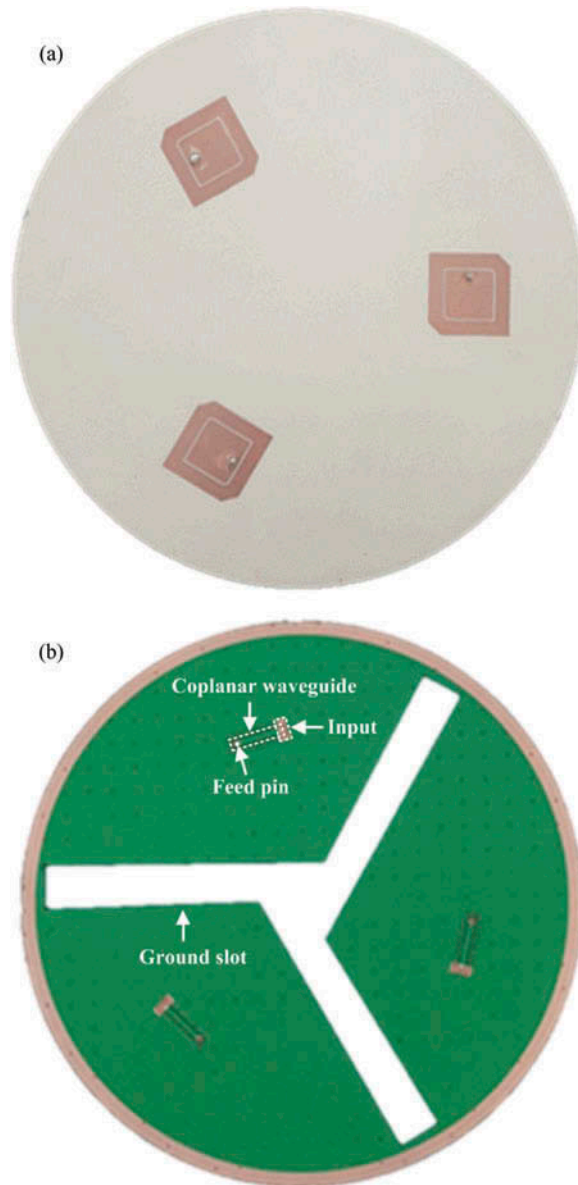


**Figure 2.** Photograph of the fabricated array: (a) Top view, (b) Bottom view.

edge length is also adjusted to maintain the impedance matching characteristics for a 50- $\Omega$  impedance. The results are then compared to those of the conventional patch antenna ( $ANT_{Conv}$ ), which has a single square patch fed by a coaxial feed. As shown in Figure 7(a),  $ANT_{Conv}$  has the maximum bandwidth of 8.1 MHz at  $h = 10$  mm, and the bandwidth becomes narrower for thicker substrates. In contrast, the proposed structure exhibits a broader bandwidth as the substrate becomes thicker ( $h > 8$  mm), and the maximum value of 11.8 MHz is observed at  $h = 12$  mm. A similar trend can also be found in the

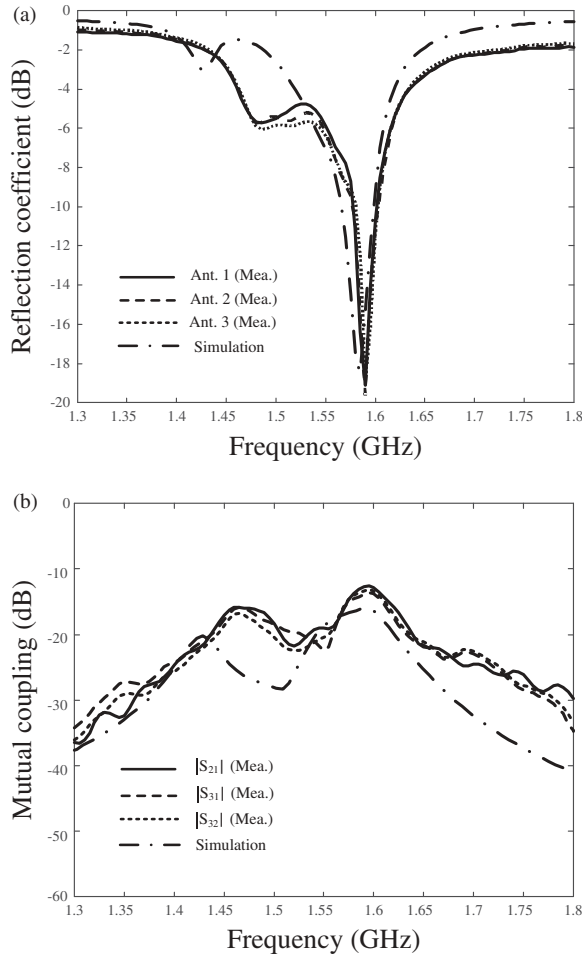


**Figure 3.** S-parameters of the proposed antenna: (a) Reflection coefficient, (b) Mutual coupling.

gain variation of Figure 7(b); for example,  $ANT_{Conv}$  shows a negative slope with the maximum value of 4.5 dBic at  $h = 5$  mm. In addition, the gain of the proposed structure is increased to the peak value of 5.3 dBic without a significant gain decrease for thicker substrates. Therefore, we can verify that the proposed structure is more suitable to achieve a broader matching bandwidth with an improved bore-sight gain, when thicker substrates are employed.

To interpret the operating principle of the proposed antenna from the circuit point of view, an equivalent circuit model is built using a data-fitting method, as shown in Figure 8(a). The feeding patch is represented by a parallel circuit of  $R_F$ ,  $L_F$ , and  $C_F$ , and the feed pin is expressed as the inductance  $L_P$ . The radiating loop is composed of  $R_L$ ,  $L_L$ , and  $C_L$ , and is connected to the circuit of the feeding patch with a series capacitance  $C_G$ . This  $C_G$  varies in accordance with the gap distance  $g$ ; for example, an increased value of  $g$  lowers the value of  $C_G$  and vice versa. Detailed values of the lumped elements are listed in Table 2, and the input impedance of the circuit is

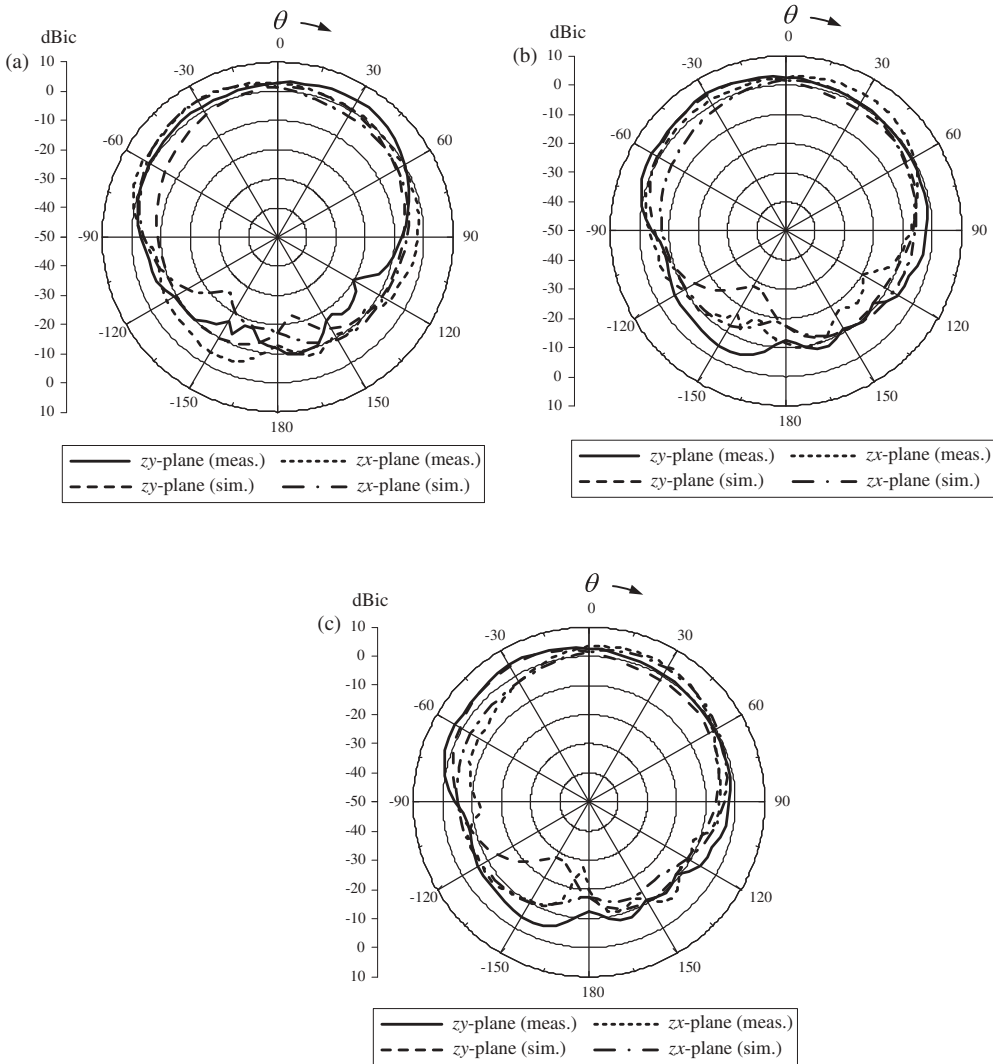
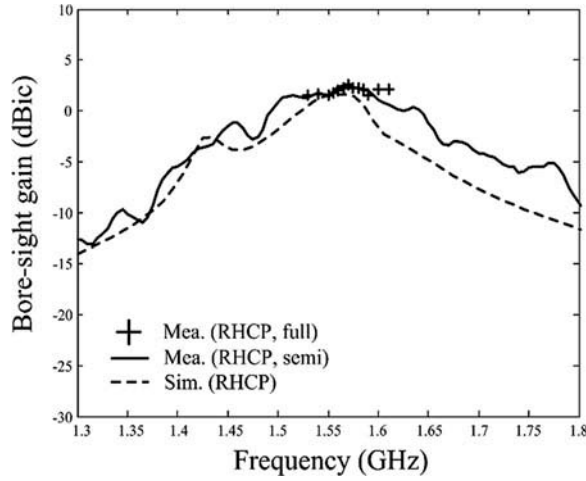


**Figure 4.** Radiation patterns of the proposed antenna: (a) Ant. 1, (b) Ant. 2, (c) Ant. 3.

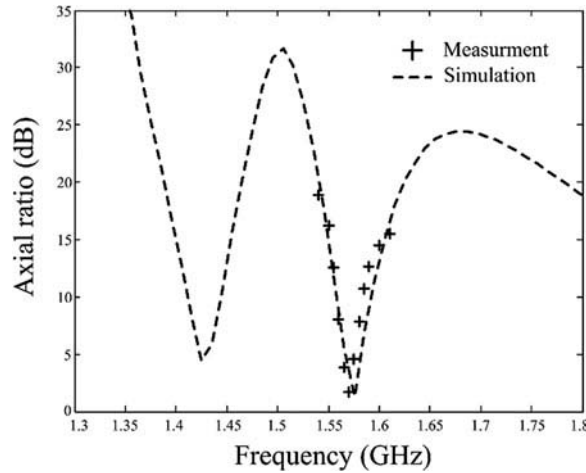
compared with that of the antenna obtained from the FEKO EM simulator, as illustrated in Figure 8(b). The solid and dotted lines indicate the resistance and reactance curves of the antenna, and the dashed and dash-dotted lines indicate those of the circuit. The results show that the input impedance of the circuit agrees well with the EM simulation, which implies that the operating principle of the proposed coupled feed structure is well described with the series capacitance  $C_G$ .

Figure 9 shows electric-field distributions of the proposed antenna at 1.5754 GHz, when an input power of 1 watt is used. The fields are observed at  $41 \times 41$  points in the  $x$ - $y$  plane at  $z = 12$  mm ( $-20$  mm  $\leq x, y \leq 20$  mm). As expected, strong electric fields are confined within the gap, which generates strong capacitance to induce electric currents to the radiating loop. Figure 10(a) shows magnetic field distributions that are





**Figure 5.** Bore-sight gain of the proposed antenna.



**Figure 6.** Axial ratio of the proposed antenna.

observed at  $37 \times 51$  points on a cross section:  $-18 \text{ mm} \leq x \leq 18 \text{ mm}$ ,  $y = 0 \text{ mm}$ ,  $0 \text{ mm} \leq z \leq 25 \text{ mm}$ . Due to the induced currents, strong magnetic fields are observed in proximity to the radiating loop with the maximum field strength of 40 dBA/m. These magnetic field distributions are averaged in the  $z$ -direction, and the results are compared to  $ANT_{Conv}$ , as shown in Figure 10(b).  $ANT_{Conv}$  has the maximum strength of 31.8 dBA/m at the center of the patch ( $x = 0$ ); on the other hand, the proposed antenna shows the peak value of 28 dBA/m at the center of the radiating loop ( $x = \pm 8 \text{ mm}$ ). In addition, the average field strength of the proposed antenna, when  $x = 15 \text{ mm}$ , is consistently lower than that of  $ANT_{Conv}$ , which helps to reduce the mutual coupling strength in small CRPA arrays.

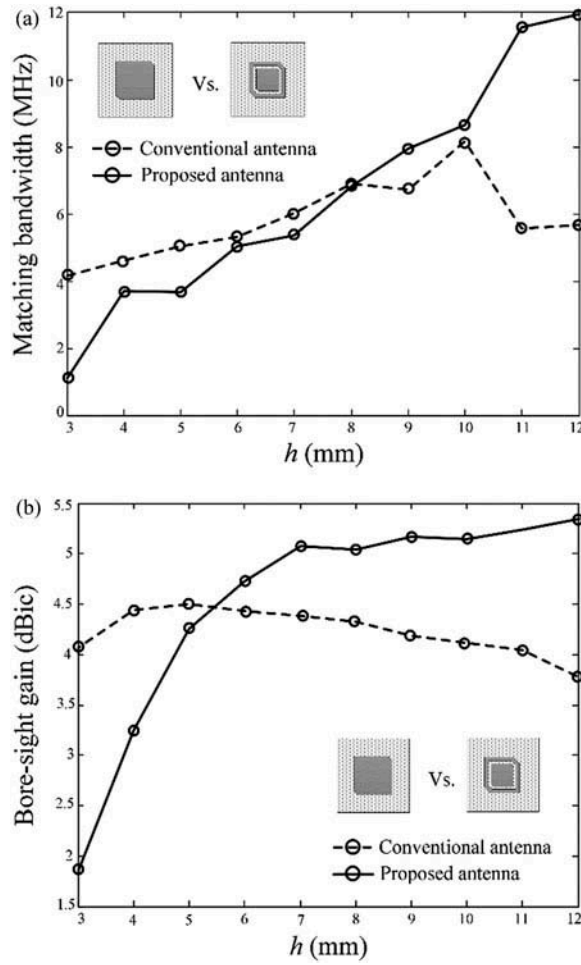


**Figure 7.** Antenna performances according to height  $h$ : (a) 10-dB matching bandwidth, (b) Bore-sight gain.

To verify the advantage of the proposed antenna in terms of the mutual coupled effect, we observe variations of the bore-sight gain and the AR of the three-element array according to the array radius  $r_2$ , as shown in Figure 11. The value of  $r_2$  is varied from 25 to 45 mm at intervals of 1 mm, while other design parameters are fixed, as specified in Table 1. The results show that the proposed array maintains a radiation gain of greater than 1 dBic and an AR of less than 3 dB up to  $r_2 = 31$  mm, which is  $0.16\lambda$ .

#### 4. Conclusion

The small CRPA array using the single-layer capacitively coupled feed structure for improved radiation gain and a broader matching bandwidth was investigated. The proposed coupled feed structure consists of an inner feeding patch and an outer radiating loop that are printed on a thick ceramic substrate. The loop is capacitively

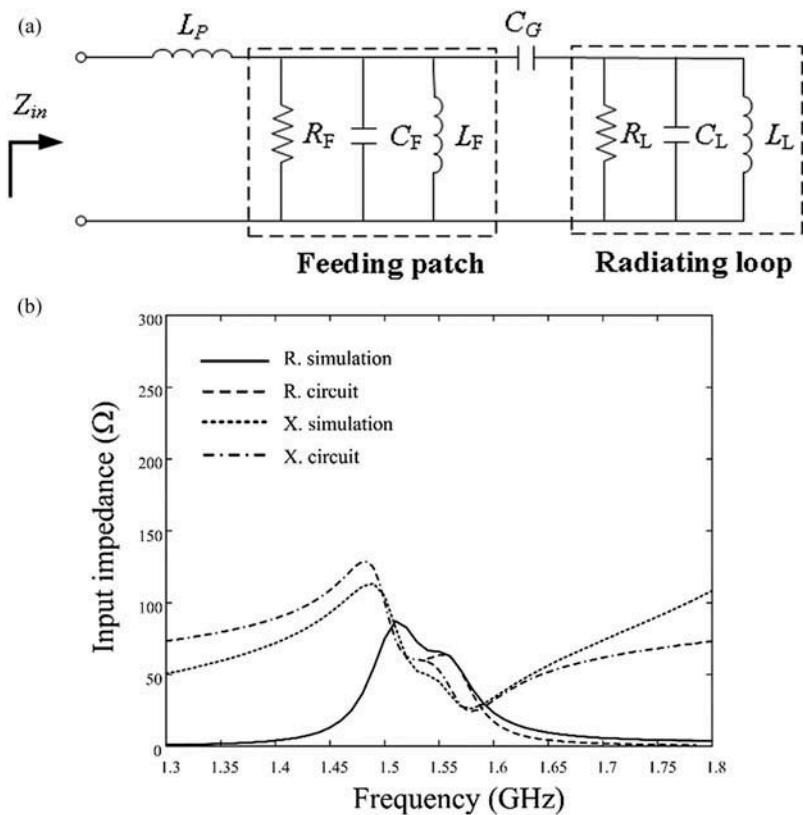


**Figure 8.** Equivalent circuit model and its input impedance: (a) Circuit model, (b) Input impedance.

**Table 2.** Parameters of the equivalent circuit

parameters	Values
$L_F$	7 nH
$R_F$	200 $\Omega$
$C_F$	26 pF
$L_F$	0.4 nH
$C_G$	1.2 pF
$R_L$	80 $\Omega$
$C_L$	25.6 pF
$L_L$	0.4 nH

coupled to the patch, and the coupling strength is adjusted by the gap distance. The proposed antenna showed a bore-sight gain of 2 dBic at 1.5754 GHz, and the 10-dB matching bandwidth was 47 MHz. The operating principle of the proposed structure was verified by building an equivalent circuit model, and antenna characteristics of the proposed antenna were compared to those of the conventional patch antenna. The results demonstrated that the proposed structure is more suitable to achieve a higher radiation gain of 5.3 dBic with the broader matching bandwidth of 11.8 MHz.

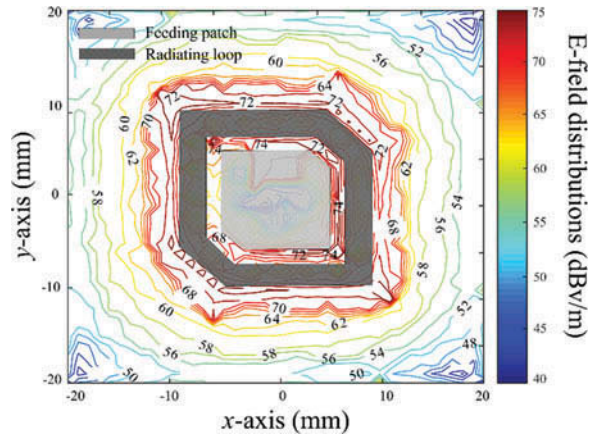


**Figure 9:** E-field distributions in  $x$ - $y$  plane ( $-20 \text{ mm} \leq x, y \leq 20 \text{ mm}$ ,  $z = 12 \text{ mm}$ ).

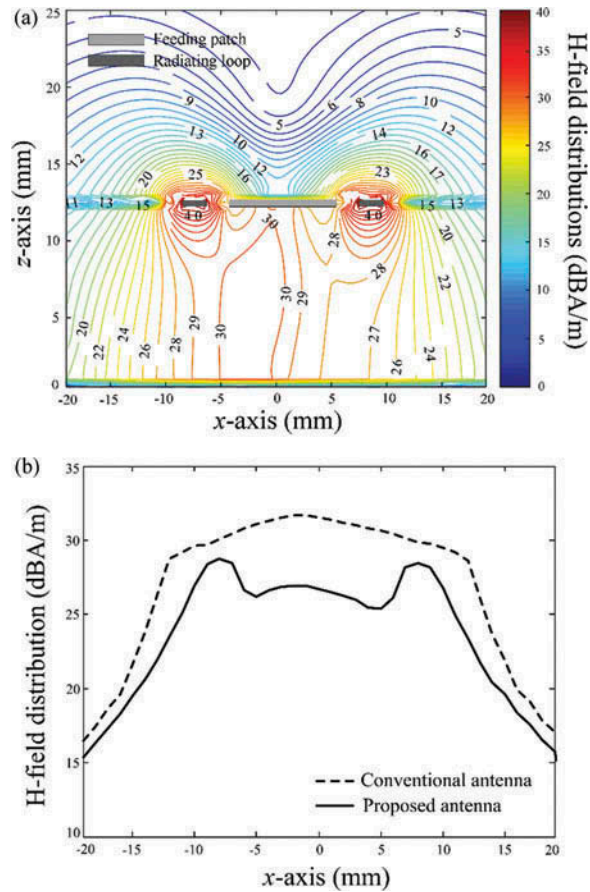


**Figure 10.** H-field distributions: (a) Fields on a cross-section ( $-18 \text{ mm} \leq x \leq 18 \text{ mm}$ ,  $y = 0 \text{ mm}$ ,  $0 \text{ mm} \leq z \leq 25 \text{ mm}$ ), (b) Average field distributions compared to *ANTConv*.

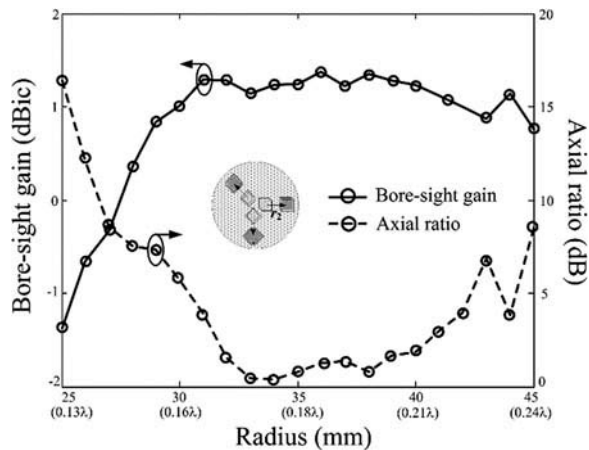


**Figure 11.** Bore-sight gain and axial ratio of Ant. 1 according to array radius  $r_2$ .

## Funding

This research was supported by the Basic Science Research Program through the National Research Foundation of Korea (NRF) funded by the Ministry of Education (No. 2015R1A6A1A03031833) and the research fund of Signal Intelligence Research Center supervised by Defense Acquisition Program Administration and Agency for Defense Development of Korea.

## References

- Bayderkhani, R., K. Forooghi, & B. Abbasi-Arand. 2015. Gain-enhanced SIW cavity-backed slot antenna with arbitrary levels of inclined polarization. *IEEE Antennas Wirel. Propag. Lett.* 14:931–934.
- Byun, G., H. Choo, & S. Kim. 2015. Improvement of pattern null depth and width using a curved array with two subarrays for CRPA systems. *IEEE Trans. Antennas Propagat.* 63:2824–2827.
- Chew D. K. C., & S. R. Saunders. 2002. Meander line technique for size reduction of quadrifilar helix antenna. *IEEE Antennas Wirel. Propag. Lett.* 1:109–111.
- FEKO. 2015. Altair Engineering, Inc., Troy, MI. Available on-line at <http://www.altair.co.kr>. (Accessed Date: November 2, 2016)
- Guo, Y.-X., L. Bian, & X.-Q. Shi. 2009. Broadband circularly polarized annular-ring microstrip antenna. *IEEE Trans. Antennas Propagat.* 57:2474–2477.
- Hebib, S., N. J. G. Fonseca, & H. Aubert. 2011. Compact printed quadrifilar helical antenna with iso-flux-shaped pattern and high cross-polarization discrimination. *IEEE Antennas Wirel. Propag. Lett.* 10:635–638.
- Kaya, A., & E.-Y. Yuksel. 2007. Investigation of a compensated rectangular microstrip antenna with negative capacitor and negative inductor for bandwidth enhancement. *IEEE Trans. Antennas Propagat.* 55:1275–1282.
- Lambert, J. R., C. A. Balanis, & D. Decarlo. 2009. Spherical cap adaptive antennas for GPS. *IEEE Trans. Antennas Propagat.* 57:406–413.
- Lee, D.-H., W.-H. Kim, D.-H. Shin, J.-C. Wang, & H. Choo. 2015. CRPA array with radiating slots for GPS applications. *Microwave Opt. Technol. Lett.* 57:1991–1995.
- Ngamjanyaporn, P., C. Phongcharoenpanich, P. Akkaraekthalin, & M. Krairiksh. 2005. Signal-to-interference ratio improvement by using a phased array antenna of switched-beam elements. *IEEE Trans. Antennas Propagat.* 53:1819–1828.
- Qu, S.-W., C.-H. Chan, & Q. Xue. 2009. Ultrawideband composite cavity-backed folded sectorial bowtie antenna with stable pattern and high gain. *IEEE Trans. Antennas Propagat.* 57:2478–2483.

- Qu, S.-W., C. H. Chan, & Q. Xue. 2010. Wideband and high-gain composite cavity-backed crossed triangular bowtie dipoles for circularly polarized radiation. *IEEE Trans. Antennas Propagat.* 58:3157–3164.
- Ramirez, M., J. Parron, M. Gonzalez, & J. Gemio. 2011. Concentric annular-ring microstrip antenna with circular polarization. *IEEE Antennas Wirel. Propag. Lett.* 10:517–519.
- Sun, Z., & P. Fay. 2006. High-gain, high-efficiency integrated cavity-backed dipole antenna at Ka-band. *IEEE Antennas Wirel. Propag. Lett.* 5:459–462.
- Zhang, Y. D., & M. G. Amin. 2011. Anti-jamming GPS receiver with reduced phase distortions. *IEEE Signal Process. Lett.* 19:635–638.